Lido for inclusive jet analysis

Wenkai Fan[1], Weiyao Ke[2] , Steffen A. Bass[1]

1. Duke University

2. University of California, Berkeley

OUTLINE

- The simulation pipeline
- The Lido transport model
- Jet and Jet Substructure
- Summary & Outlook

Introducing the Quark Medium Plasma – Collision and Pre-equlibrium

AuAu collision @ 200GeV, figure credit: Hannah Petersen

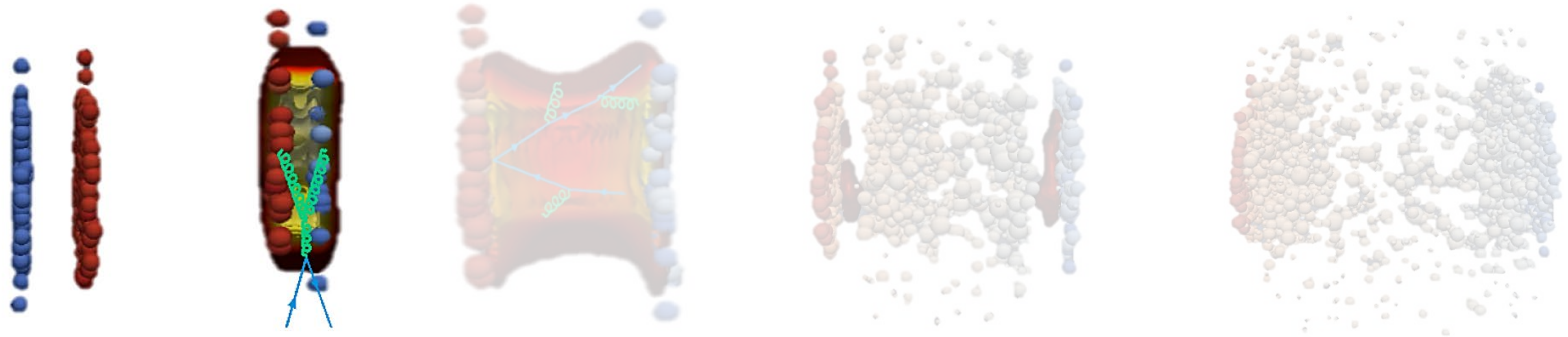

Soft matter:

- Multiple nucleon collision
- TRENTO: parametrized entropy deposition
- Free streaming approximation

Hard parton:

- TRENTO: sample nucleon positions
- Momentum distribution: Pythia with nuclear PDF
- Free streaming approximation

Introducing the Quark Medium Plasma – Hydrodynamical expansion

AuAu collision @ 200GeV, figure credit: Hannah Petersen

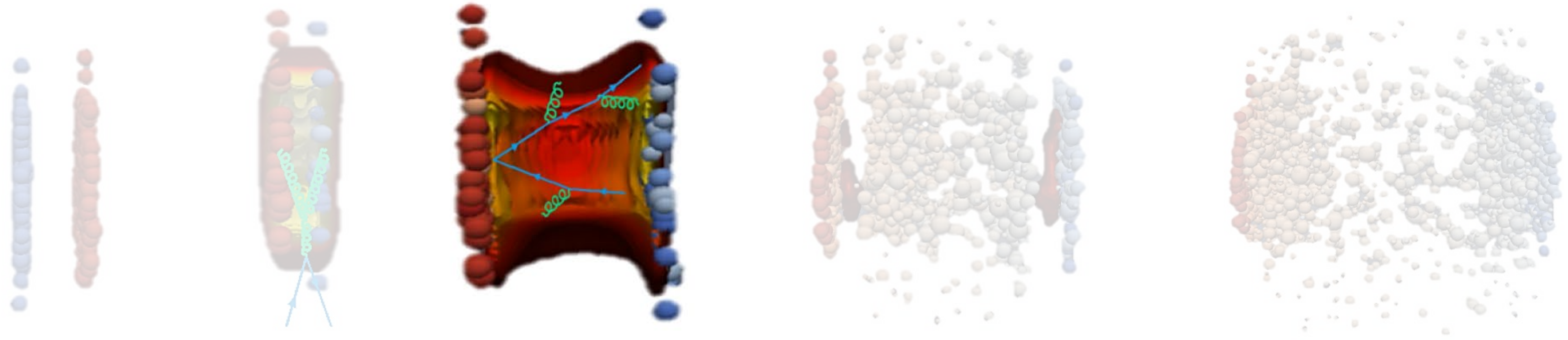

Soft matter:

- Hydrodynamical expansion
- Near local equilibrium
- Equation of State from Lattice QCD
- Shear and bulk viscosity $\frac{\eta}{s}(T), \frac{\zeta}{s}(T)$

Hard parton:

- Transport models - Lido
- Collisional & radiational energy loss

  -> jet quenching

Introducing the Quark Medium Plasma – Hadronization and Rescattering

AuAu collision @ 200GeV, figure credit: Hannah Petersen

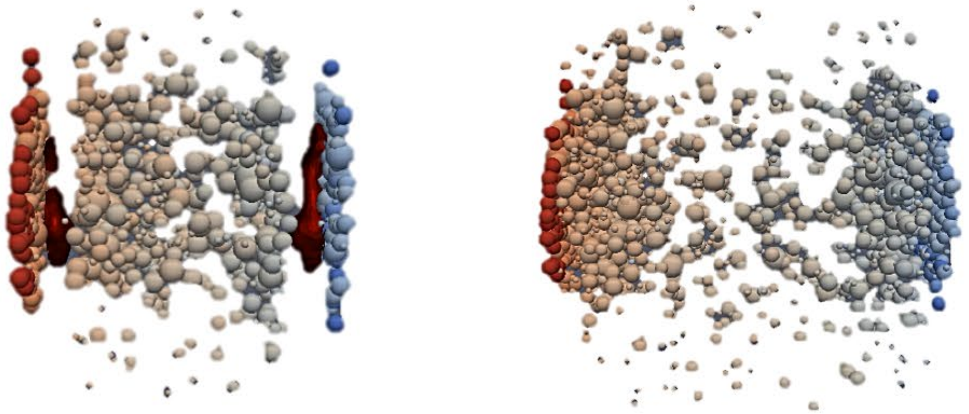

Soft matter:

- Particlization at T_{switch}
- Hadronic rescattering (UrQMD)

Hard parton:

- Recombination + fragmentation
- Hadronic rescattering (UrQMD)

Lido Transport Model - Interactions

The evolution of hard parton distribution functions are described by Boltzmann transport equation:

$$\frac{df}{dt} = \mathcal{D}[f] + \mathcal{C}^{1\leftrightarrow 2}[f] + \mathcal{C}^{2\leftrightarrow 2}[f] + \mathcal{C}^{2\leftrightarrow 3}[f]$$

We further divide the interaction kernels into large and small momentum transfer q ones, where the switching scale Q_{cut} should obey $gT \ll Q_{cut} \ll T$.

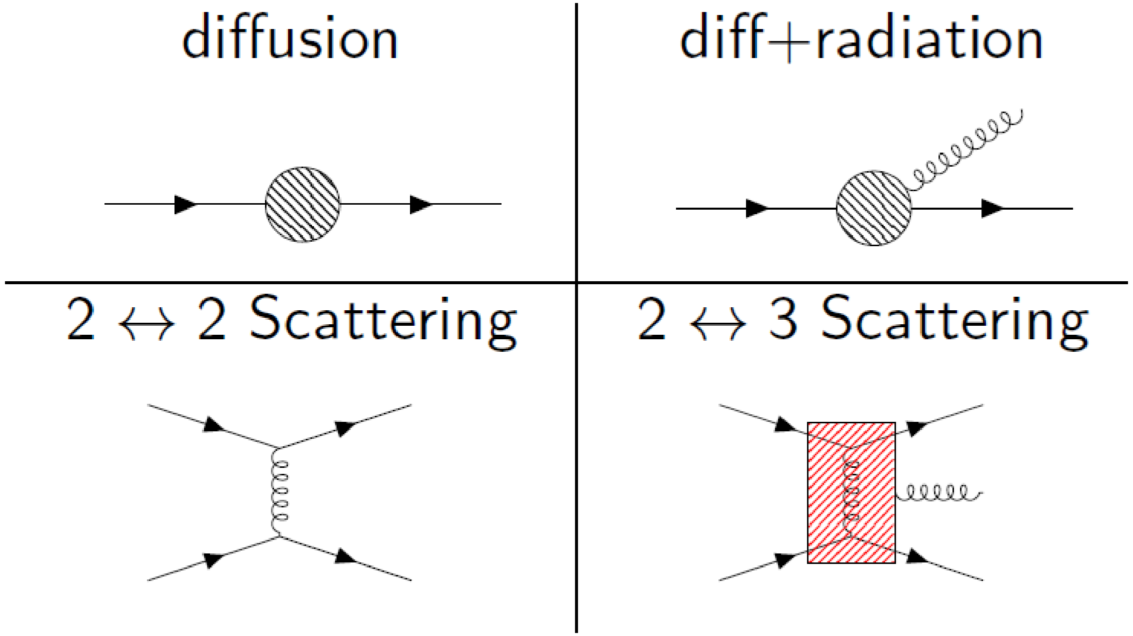

Ke, Weiyao, Yingru Xu, and Steffen A. Bass. arXiv:1810.08177 (2018).

Lido Transport Model - Interactions

1. Elastic and large q collisions (vacuum QCD matrix element)

$$R = \frac{g_i}{2E_1}\int \frac{d^3p_2}{2E_2(2\pi)^3} f_0(p_2) 2\hat{s} \sum_i \int_{-\hat{s}}^{0} \frac{d\sigma_i}{d\hat{t}} d\hat{t}$$

2. Elastic and small q diffusion

$$\begin{cases} \dfrac{dx_i}{dt} = \dfrac{p_i}{E} \\ \dfrac{dp_i}{dt} = -\eta_D p_i + \xi_i(t) \end{cases}$$

3. Inelastic and large q collisions

The matrix elements for 2 $\rightarrow$ 3 processes are derived under the limits $k, q \ll \sqrt{s}$.

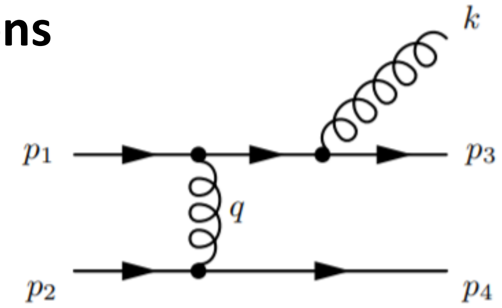

4. Inelastic and small q collisions

$$R_{1\to 2} = \kappa_T \int d\boldsymbol{k}^2\, dx \frac{\alpha_s P(x)}{2\pi\left(\boldsymbol{k}^2 + m_D^2/2\right)}$$

The reverse inelastic process rates $\mathrm{R}_{3\to 2}$ and $\mathrm{R}_{2\to 1}$ can be written down by the requirement of detailed balance but are omitted in the current setup due to their small contribution to the total collision rate.

PART 2

Lido Transport Model – The LPM Effect

The formation time for a certain splitting is

$$\tau_f \approx \frac{2}{\omega\theta^2}$$

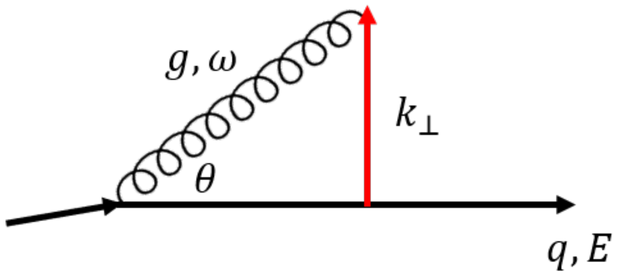

τ_f can be much bigger than the mean free path $\lambda \approx 1/g^2 T$ for **hard and colinear** splitting.

- When this is the case, theoretical calculations indicates the radiation rate is suppressed by a factor proportional to λ/τ_f (deep LPM regime) compared to the incoherent limit.
- When formation time is short, the incoherent limit rate recovers and is called the Bethe-Heitler regime.
- Need a Monte-Carlo method that interpolates these two regimes and can be extended to a dynamic medium.

PART 2

Lido Transport Model – The LPM Effect

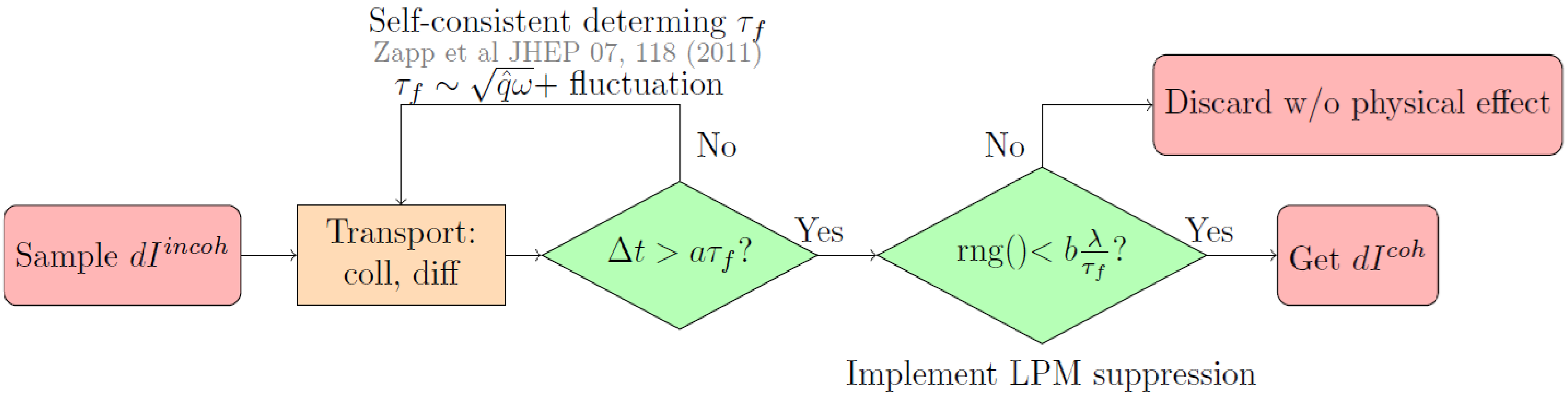

A “non-local” Boltzmann Equation. Figure credit: Weiyao Ke

(The factors a and b are used to match to NLL calculations in a infinite medium)

PART 2

Lido Transport Model – The LPM Effect

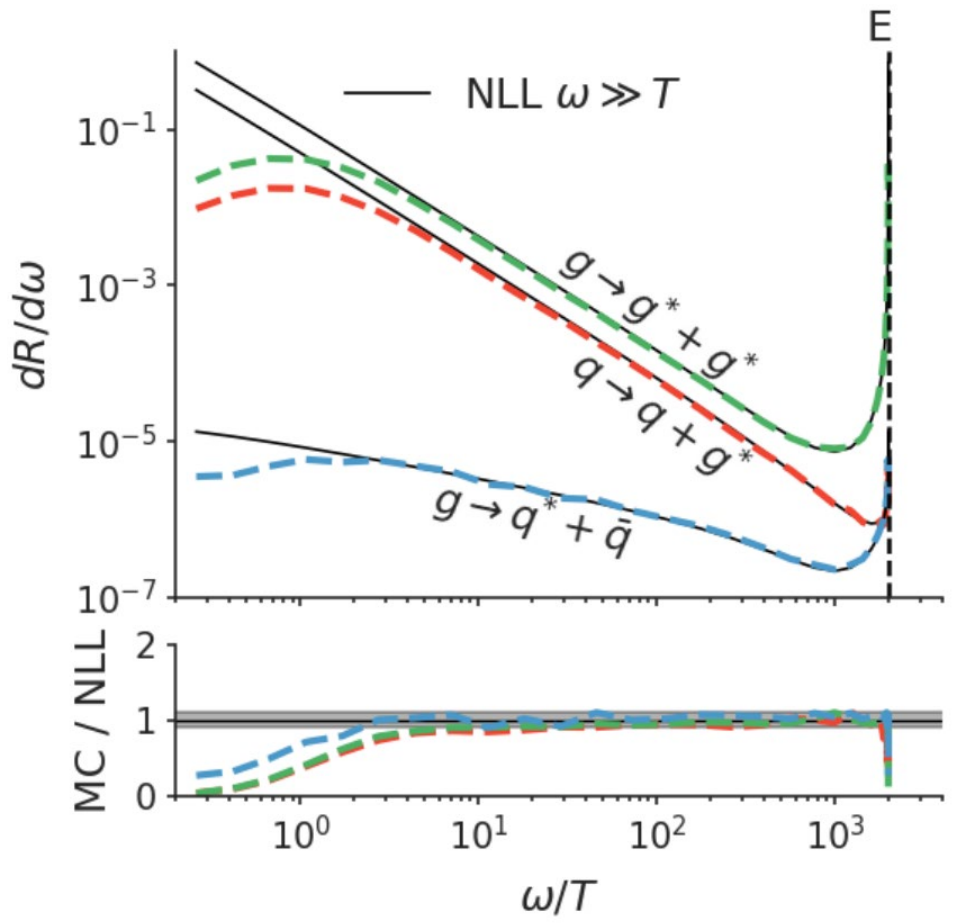

Comparison with AMY formalism in an infinite medium

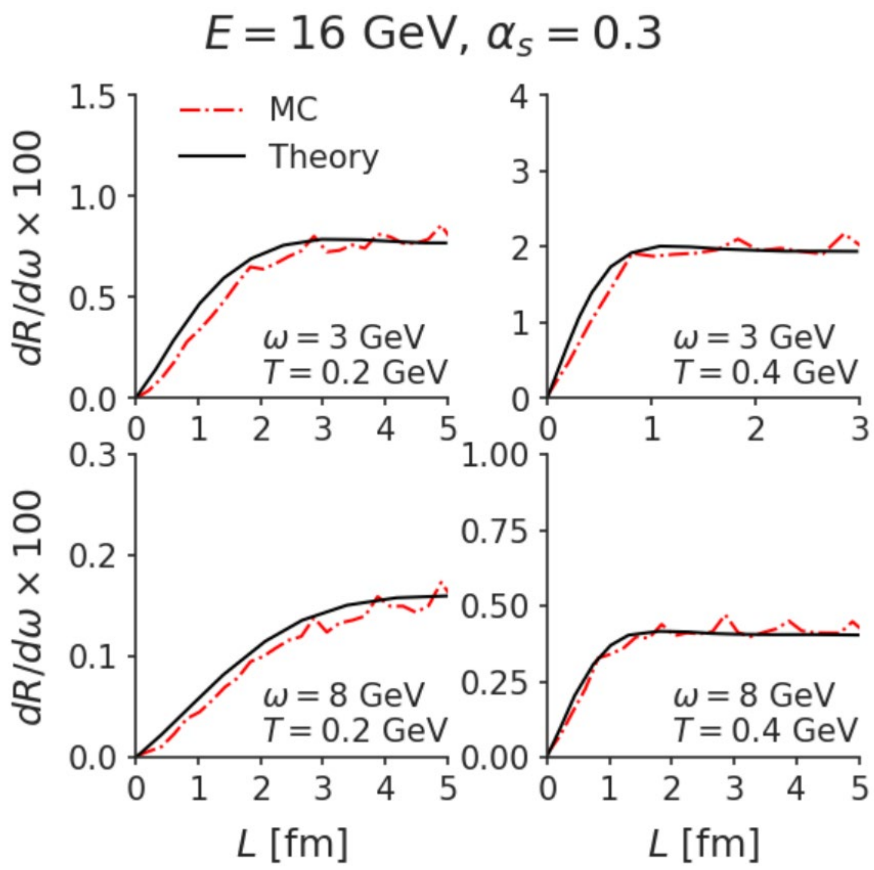

Splitting rate in a finite medium

PART 2

Lido Transport Model – Open-Heavy Flavor Results

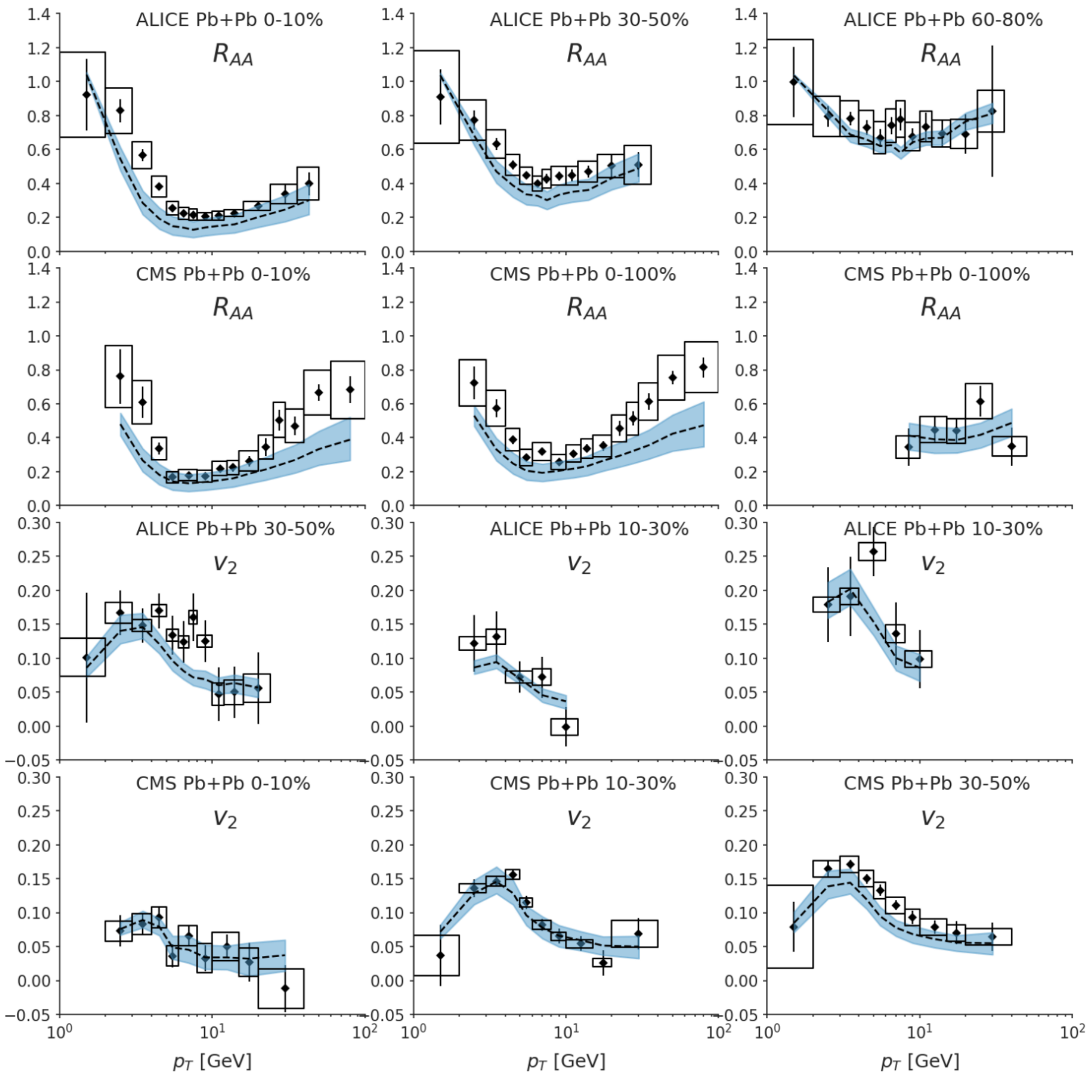

Calibrated results on open heavy flavor observables

Ke, Weiyao. arXiv preprint arXiv:2001.02766 (2020).

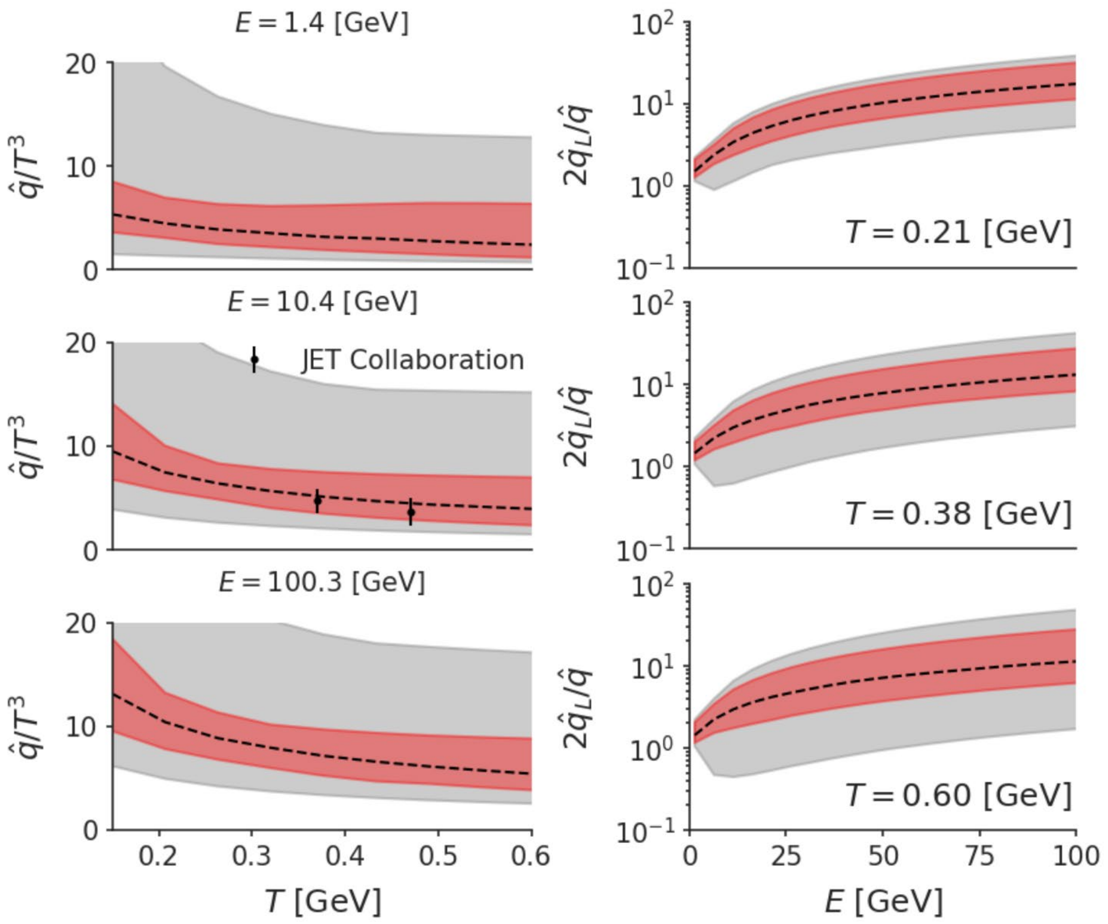

90% CL of transport coefficients

Jet and Jet Substructure – Jet Substructure

Jet shape:

$$\rho(r) = \frac{1}{\delta r}\frac{1}{N_{jet}}\sum_{jets}\frac{\sum_i p_{i,T}}{p_T^{jet}}$$

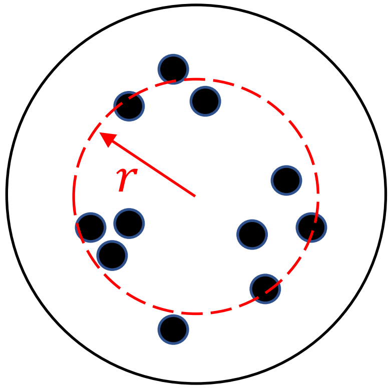

Dijet asymmetry:

$$A_J = \frac{p_{T1} - p_{T2}}{p_{T1} + p_{T2}}, \Delta\phi > \frac{\pi}{2}$$

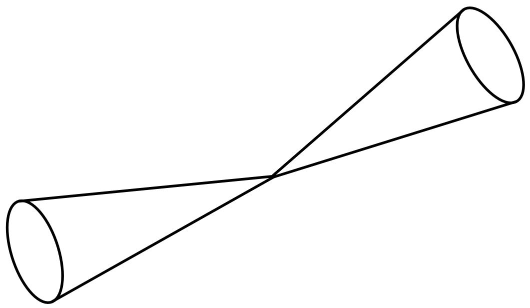

Jet fragmentation function:

$$z = p_T cos\Delta R / p_T^{jet}$$

$$D(z) = \frac{1}{N_{jet}}\frac{dn_{ch}}{dz}$$

$$D(p_T) = \frac{1}{N_{jet}}\frac{dn_{ch}}{dp_T}$$

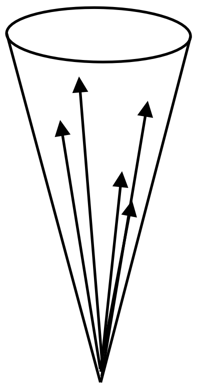

Z/γ tagged jets:

$$\frac{1}{N_v}\frac{dN_{jv}}{dx_{jv}}$$

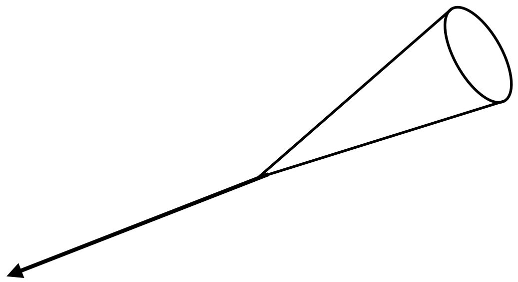

PART 3

Jet and Jet Substructure – Preliminary results

The hydrodynamic simulation is event-averaged and jets are clustered at the parton level. We also compare the results with recoil partons from the medium and without.

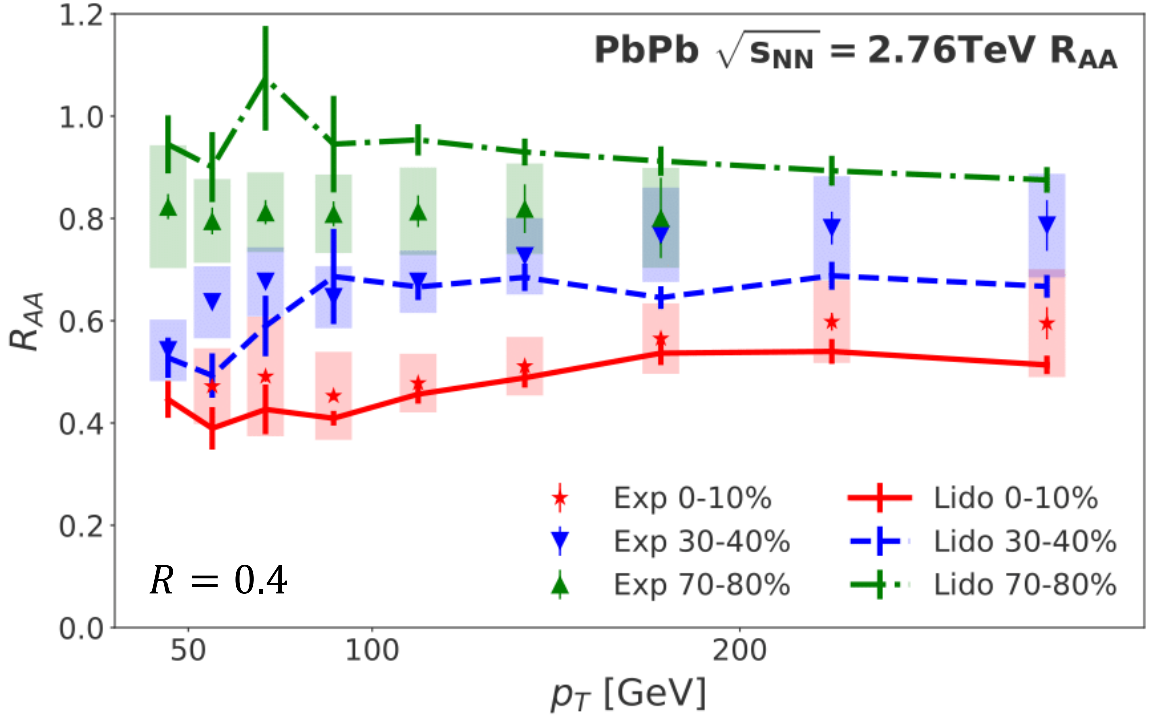

R_{AA} *with recoil*

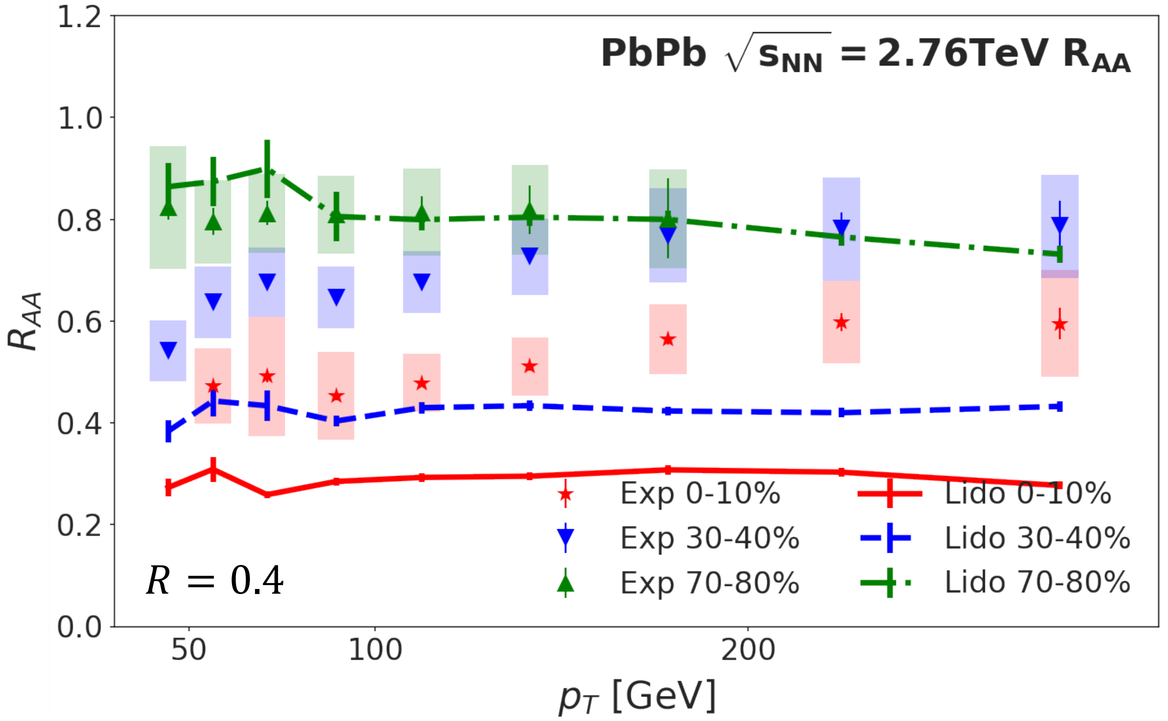

R_{AA} *without recoil*

Jet and Jet Substructure – Preliminary results – no recoil

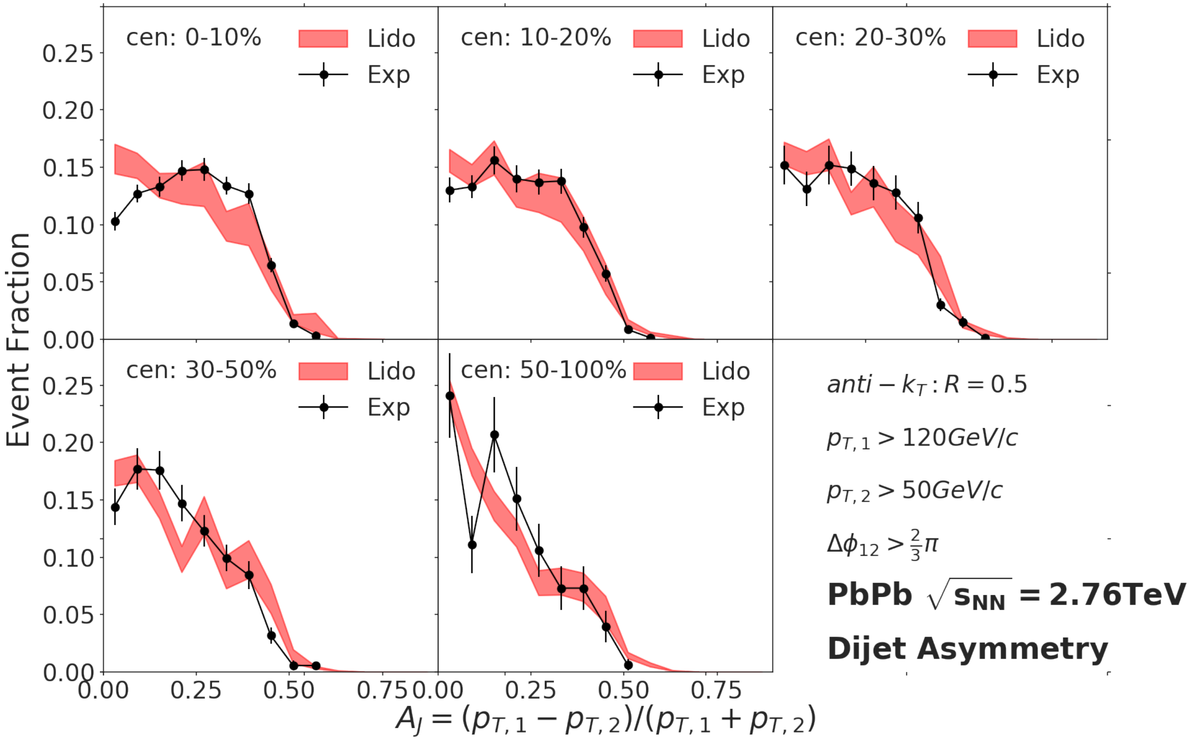

Dijet asymmetry with recoil

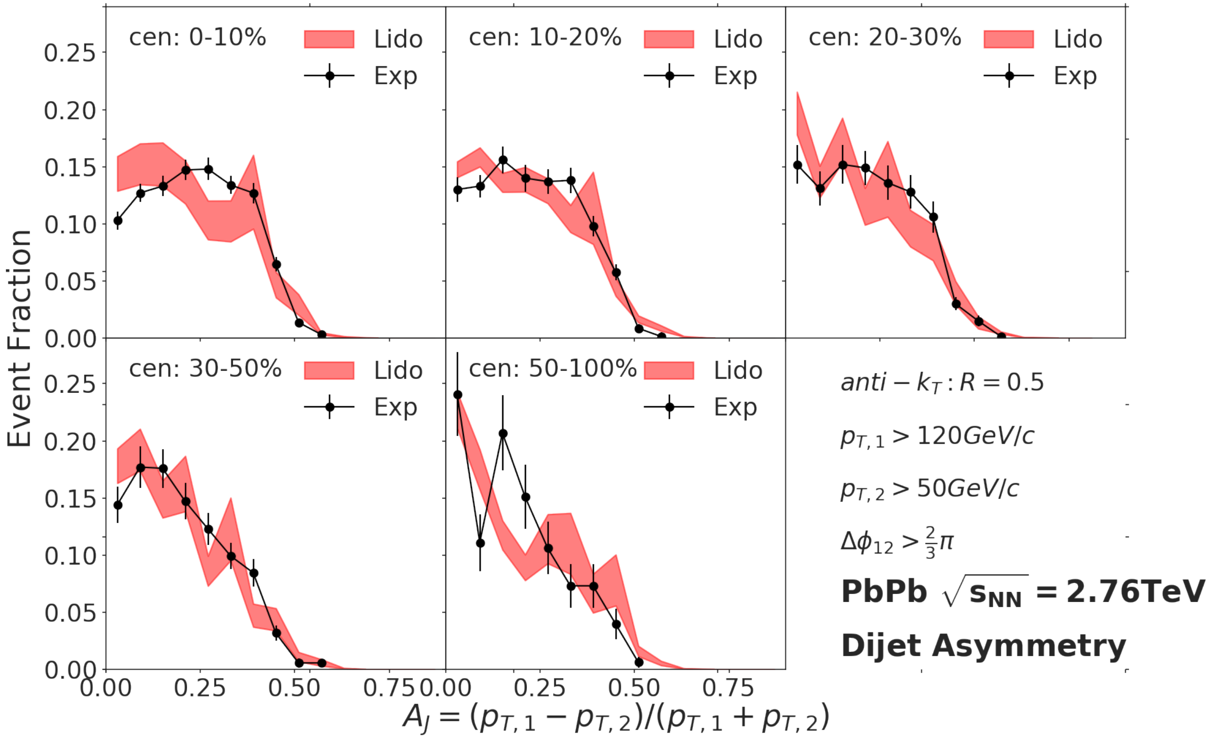

Dijet asymmetry without recoil

PART 3

Jet and Jet Substructure – Preliminary results

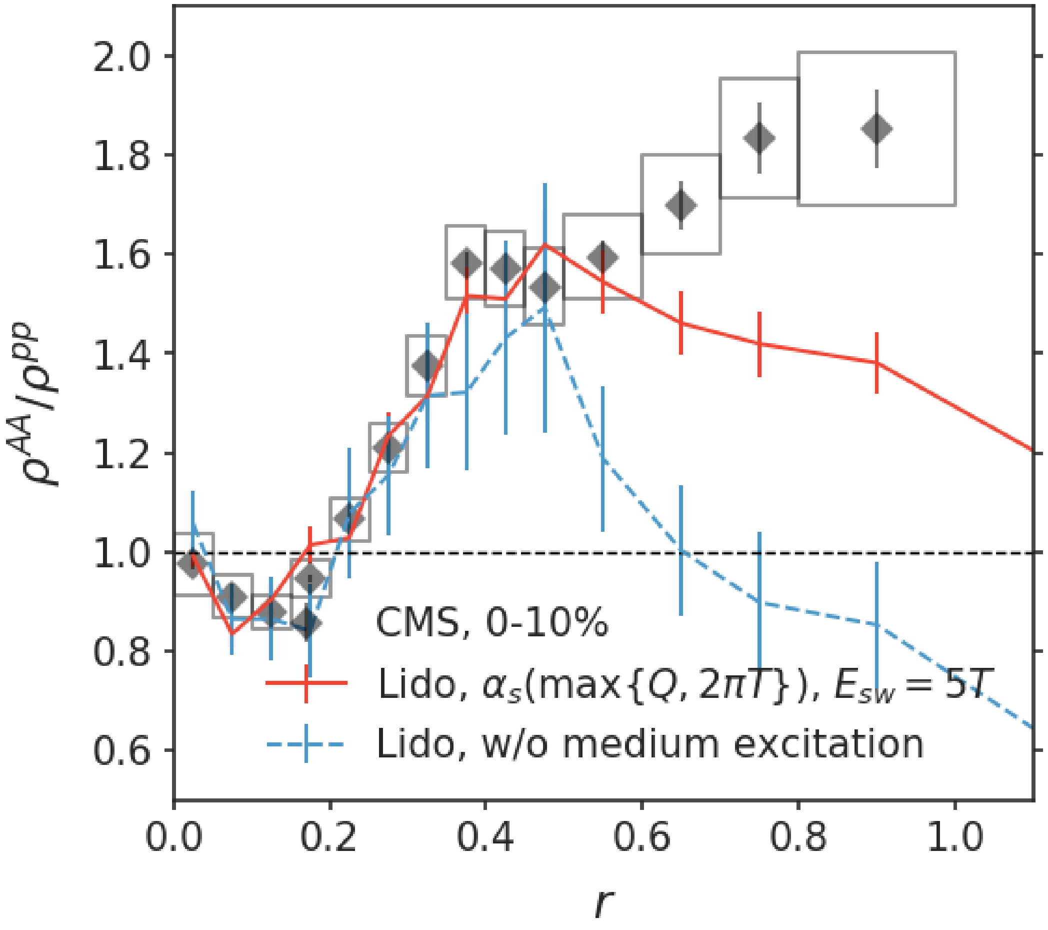

Preliminary W Ke, XN Wang, work in progress

PART 4

Summary & Outlook

- Lido is a hybrid transport model for both **light** and **heavy** parton transport.
- Jet observables are powerful tools for probing the QGP medium which reveal both longitudinal and transversal parton-medium interactions.
- Considering the progress we are making, we think it is a promising project towards **heavy jet** analysis.
- After including *event-by-event hydro, medium response, hadronization and background subtraction*, we will apply a Bayesian analysis on the transport coefficients and compare with previous results.
- Adaption of JETSCAPE 3.0 in the near future.

Thank you!

Jet and Jet Substructure – What is a Jet?

- Collimated ensemble of highly energetic particles usually created by initial hard scatterings
- Reconstructed by jet algorithm
- Quenching (energy loss) observed → QGP transport properties

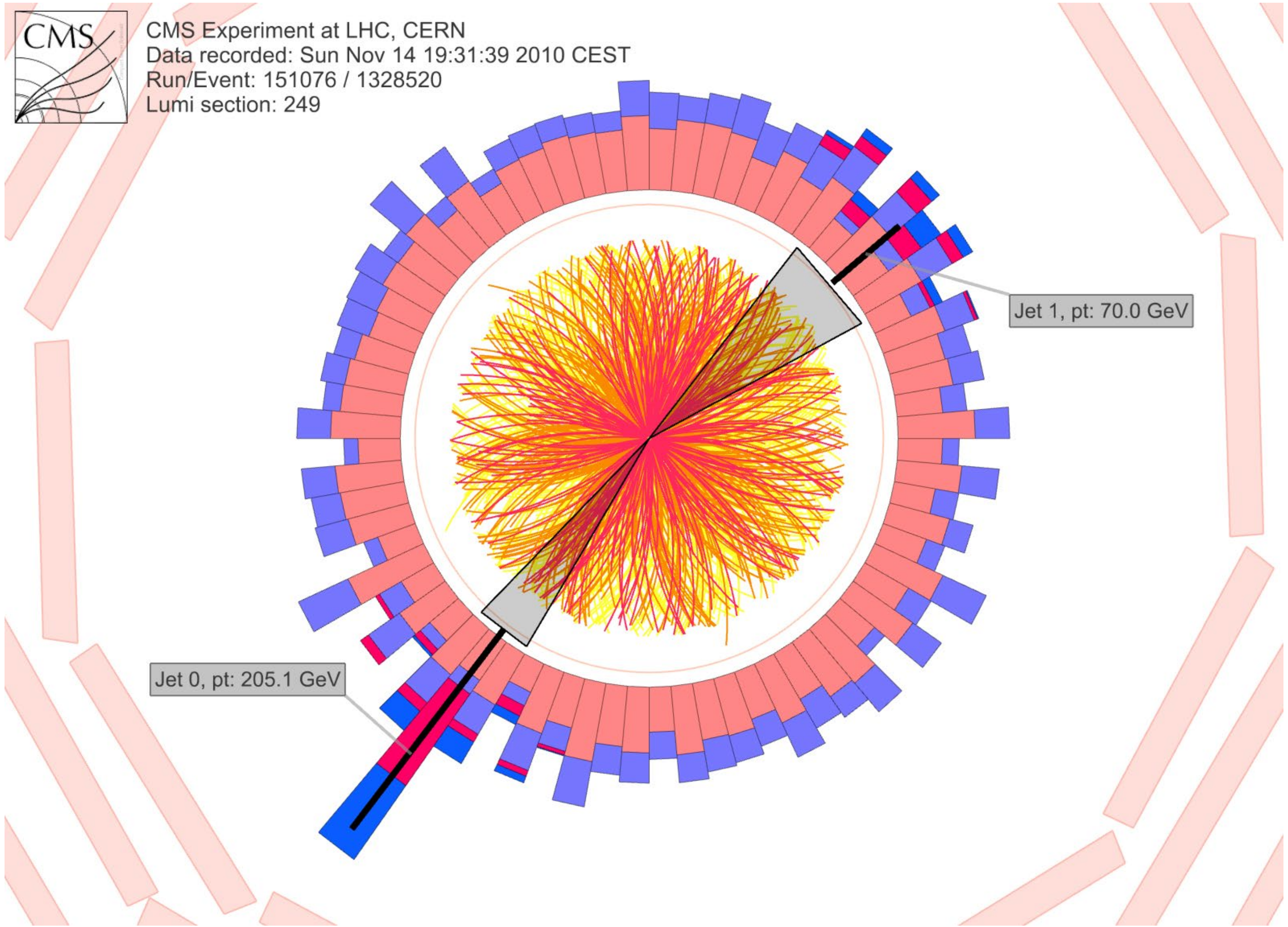

Jet and Jet Substructure – Jet Algorithm

Jet algorithms should be infra-red safe and collinear safe. We adopt the sequential clustering algorithm:

- d_{ij} (distance between particle i and particle j) and d_{iB} (distance between particle i and beam B) are defined as:

$$d_{ij} = \min\left(k_{\perp i}^{2p}, k_{\perp j}^{2p}\right)\frac{\Delta_{ij}^2}{R^2}$$
$$d_{iB} = k_{\perp i}^{2p}$$

where $\Delta_{ij} = \left(y_i - y_j\right)^2 + \left(\phi_i - \phi_j\right)^2$, $k_{\perp i}$ is the transverse momentum, y_i is the rapidity and ϕ_i is the azimuthal angle.

- p is a input parameter, $p = 1$ is the k_T algorithm, $p = 0$ is the Cambridge/Aachen algorithm and $p = -1$ is the anti-k_T algorithm.

- At each step, the minimum among all the values of d_{ij} and d_{iB} is found. If the smallest element is d_{ij}, combine i and j. If the smallest element is d_{iB}, i is labeled as a jet and removed from the list.

Jet and Jet Substructure – Nuclear modification factor/Background subtraction

Nuclear modification factor:

$$R_{AA}^{jet} = \frac{\left.\frac{d^2N_{jet}}{dp_T dy}\right|_{AA}}{< N_{bin} > \left.\frac{d^2N_{jet}}{dp_T dy}\right|_{pp}}$$

Nuclear modified jet shape:

$$\rho_{AA}(r)/\ \rho_{pp}(r)$$

Because there are soft contributions from the bulk medium within the jet cone that we are generally not interested, background subtraction are often required to remove those low p_T particles (jet grooming and re-clustering are also used in experimental analysis). However the implementations might differ for different experiments. How to ensure an apple-to-apple comparison with experiments is what we need to pay attention to.

Lido Transport Model - Interactions

1. Elastic and large q collisions

$$R = \frac{g_i}{2E_1}\int \frac{d^3p_2}{2E_2(2\pi)^3} f_0(p_2) 2\,\hat{s} \sum_i \int_{-\hat{s}}^{0} \frac{d\sigma_i}{d\hat{t}} d\hat{t}$$

2. Elastic and small q diffusion

$$\begin{cases} \dfrac{dx_i}{dt} = \dfrac{p_i}{E} \\ \dfrac{dp_i}{dt} = -\eta_D p_i + \xi_i(t) \end{cases}$$

where $\langle \xi_i(t) \rangle = 0$, $\langle \xi_i(t)\xi_j(t') \rangle = (\kappa_L \frac{p_i p_j}{p^2} + \kappa_T \left(\delta_{ij} - \frac{p_i p_j}{p^2}\right))\delta(t - t')$

$$\kappa_T = \int_0^{Q_{cut}^2} dq^2 \frac{\alpha_s m_D^2 T}{q^2(q^2 + m_D^2)} \qquad \kappa_L = \int_0^{Q_{cut}^2} dq^2 \frac{\alpha_s (m_D^2/2) T}{q^2(q^2 + m_D^2/2)} \qquad \eta_D = \frac{\kappa_L}{2ET} - \frac{\kappa_L - \kappa_T}{p^2} - \frac{\partial \kappa_L}{\partial p^2}$$

APPENDIX

Lido Transport Model - Interactions

3. Inelastic and large q collisions

The matrix elements for $2 \to 3$ processes are derived under the limits $k, q \ll \sqrt{s}$ and can be found in the appendix.

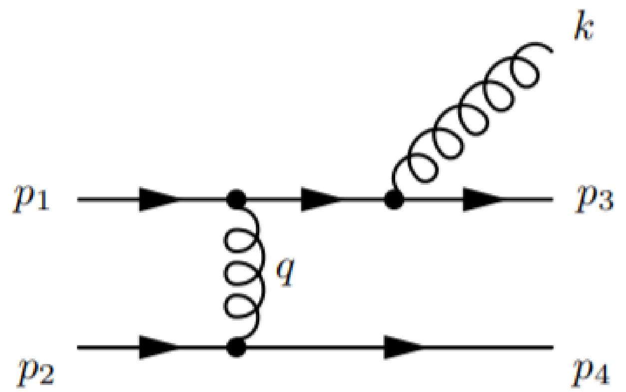

4. Inelastic and small q collisions

$$R_{1\to2} = \kappa_T \int d\boldsymbol{k}^2\, dx \frac{\alpha_s P(x)}{2\pi\left(\boldsymbol{k}^2 + m_D^2/2\right)}$$

The reverse inelastic process rates $\mathrm{R}_{3\to2}$ and $\mathrm{R}_{2\to1}$ can be written down by the requirement of detailed balance but are omitted in the current setup due to their small contribution to the total collision rate.

APPENDIX

Lido Transport Model – The LPM Effect

1. When a splitting happens at t_0, final state partons b and c are not immediately treated as physical objects to the system. The parent parton can carry arbitrary numbers of such “preformed” final-state copies.
2. Evolve from t to $t + \Delta t$ the “preformed” final state partons in each copy with only elastic processes. While the parent parton is evolved under the full Boltzmann equation.
3. Recalculate formation time τ_f for those “preformed” partons after each time step.
4. Repeat steps 1 to 3 until $t - t_0 > a\tau_f(t)$ is satisfied.
5. Then, the “preformed” final state is considered to become the physical final state with probability $p = min\{1, \frac{ab\lambda(t)}{\tau_f}\}$.

(The factors a and b are used to match to NLL calculations in a infinite medium)

APPENDIX $2 \to 2$ *processes*

Light parton scattering:

$$\overline{|M_{q_1 q_2 \to q_1 q_2}|^2} = \frac{64\pi^2\alpha_s^2}{9}\frac{s^2+u^2}{t^2}$$

$$\overline{|M_{gg \to gg}|^2} \approx 72\pi^2\alpha_s^2\frac{-su}{t^2}$$

$$\overline{|M_{qg \to qg}|^2} \approx 16\pi^2\alpha_s^2\frac{s^2+u^2}{t^2}$$

Heavy parton scattering:

$$\overline{|M_{Qq \to Qq}|^2} = \frac{64\pi^2\alpha_s^2}{9}\frac{(M^2-u)^2+(s-M^2)^2+2M^2t}{t^2}$$

$$\begin{aligned}\overline{|M_{Qq \to Qq}|^2} = \pi^2 \Bigg\{ & 32\alpha_s^2\frac{(s-M^2)(M^2-u)}{t^2} \\ + & \frac{64}{9}\alpha_s^2\frac{(s-M^2)(M^2-u)+2M^2(s+M^2)}{(s-M^2)^2} \\ + & \frac{64}{9}\alpha_s^2\frac{(s-M^2)(M^2-u)+2M^2(u+M^2)}{(M^2-u)^2} \\ + & \frac{16}{9}\alpha_s^2\frac{M^2(4M^2-t)}{(M^2-u)(s-M^2)} \\ + & 16\alpha_s^2\frac{(s-M^2)(M^2-u)+M^2(s-u)}{t(s-M^2)} \\ - & 16\alpha_s^2\frac{(s-M^2)(M^2-u)-M^2(s-u)}{t(M^2-u)} \Bigg\}\end{aligned}$$

APPENDIX

$2 \to 3$ *processes*

Colinear approximation: $k_\perp^2, q_\perp^2 \ll x(1-x)\hat{s}\ , x = k^+/\sqrt{s}$

The matrix-element is factorized into an amplitude for the splitting process (approximated in the collinear limit) times the amplitude for two-body collision with the medium parton.

$$\begin{aligned}
\overline{|M^2|}_{g+i\to g+g+i} &= \overline{|M^2|}_{g+i\to g+i} P_{gg}^{g(0)} D_{gg}^{g}, \\
\overline{|M^2|}_{g+i\to q+\bar{q}+i} &= \frac{C_F d_F}{C_A d_A} \overline{|M^2|}_{g+i\to g+i} P_{q\bar{q}}^{g(0)} D_{q\bar{q}}^{g}, \\
\overline{|M^2|}_{q+i\to q+g+i} &= \overline{|M^2|}_{q+i\to q+i} P_{qg}^{q(0)} D_{qg}^{q}.
\end{aligned}$$

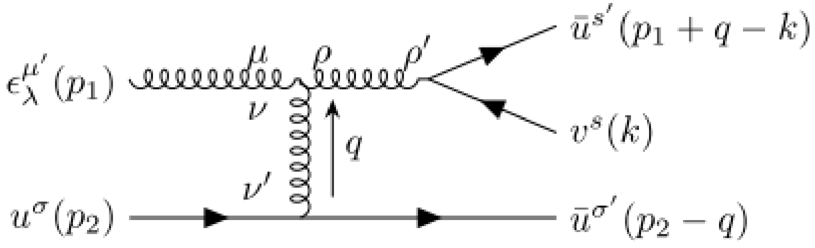

$$\begin{aligned}
P_{gg}^{g(0)} &= g^2 C_A \frac{1+x^4+(1-x)^4}{x(1-x)}, \\
P_{qg}^{q(0)} &= g^2 C_F \frac{1+(1-x)^4}{x}, \\
P_{q\bar{q}}^{g(0)} &= g^2 \frac{N_f}{2}\left(x^2+(1-x)^4\right).
\end{aligned}$$

$$\begin{aligned}
D_{qq}^{g} &= C_A(\mathbf{a}-\mathbf{b})^2 + C_A(\mathbf{a}-\mathbf{b})^2 \\
&- C_A(\mathbf{a}-\mathbf{b})\cdot(\mathbf{a}-\mathbf{c}), \\
D_{q\bar{q}}^{g} &= C_F(\mathbf{a}-\mathbf{b})^2 + C_F(\mathbf{a}-\mathbf{b})^2 \\
&- (2C_F - C_A)(\mathbf{a}-\mathbf{b})\cdot(\mathbf{a}-\mathbf{b}), \\
D_{qg}^{q} &= C_F(\mathbf{c}-\mathbf{a})^2 + C_F(\mathbf{c}-\mathbf{b})^2 \\
&- (2C_F - C_A)(\mathbf{c}-\mathbf{a})\cdot(\mathbf{c}-\mathbf{b}).
\end{aligned}$$

$$\mathbf{a} = \frac{\mathbf{k}-x\mathbf{q}}{(\mathbf{k}-x\mathbf{q})^2}, \mathbf{b} = \frac{\mathbf{k}-\mathbf{q}}{(\mathbf{k}-\mathbf{q})^2}, \mathbf{c} = \frac{\mathbf{k}}{\mathbf{k}^2}.$$

Factorization

$$\sigma^{AB\to X+jet} = \sum_{abcd} f_A(x_a, Q_f) \otimes f_B(x_b, Q_f) \otimes \sigma_{ab\to cd}(x_a, x_b, Q_R)$$

$$\sigma^{AB\to X+jet} = \int_{geometry} \sum_{abcd} f'_A(x_a, Q_f) \otimes f'_B(x_b, Q_f) \otimes \sigma_{ab\to cd}(x_a, x_b, Q_R) \otimes \mathrm{P}(x_c \to x'_c \,|T, u^\tau)$$

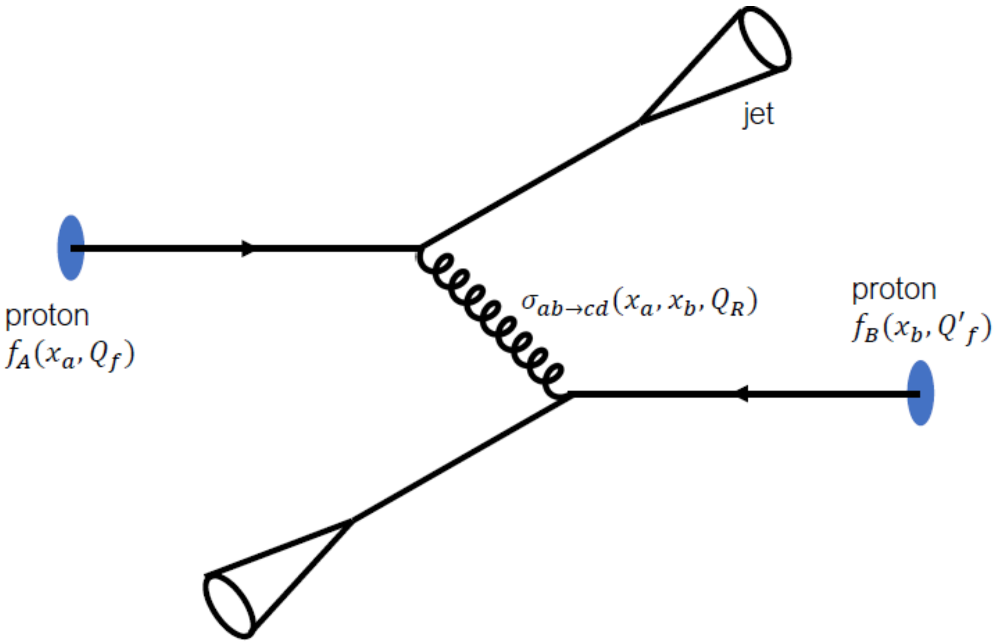

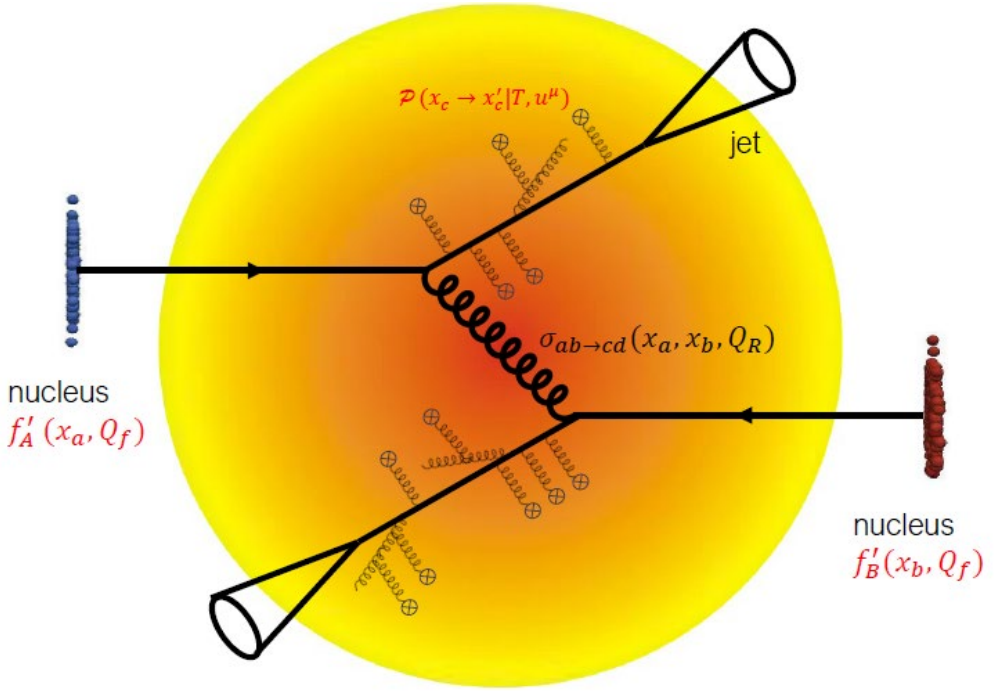

Q_{cut} dependence

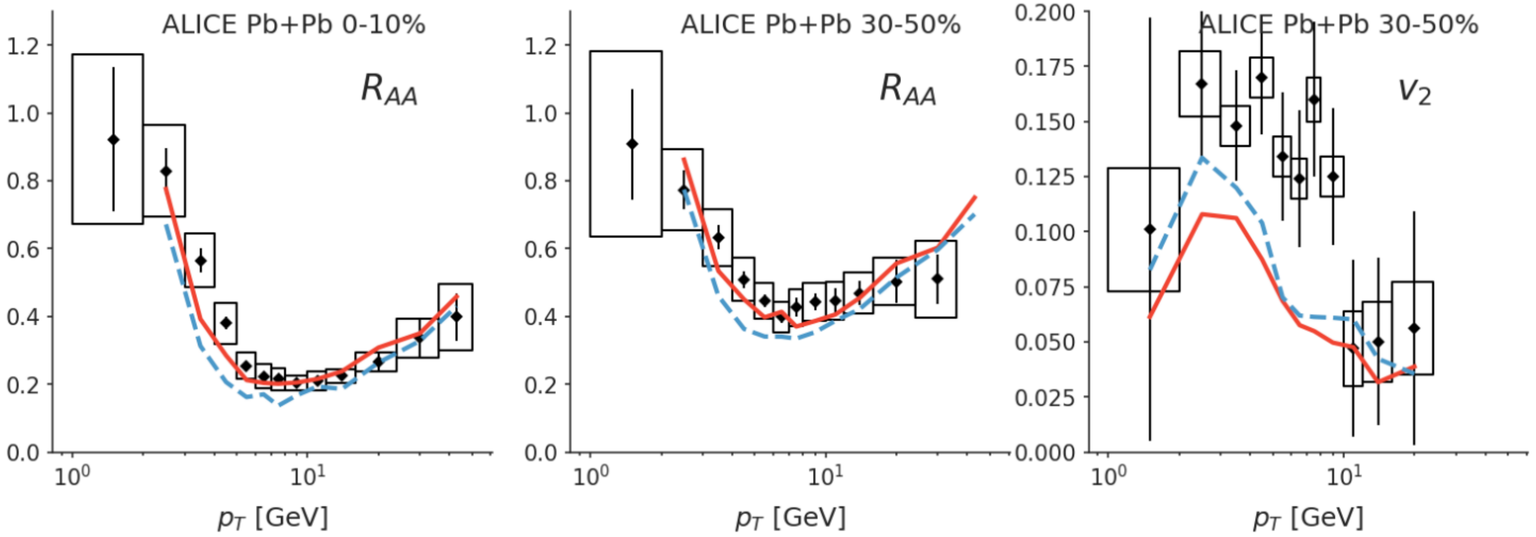

Figure 4.9 Effect of changing the switch scale between small-Q diffusion modeling and large-Q scattering modeling. $\mu = 2$ is used. The red solid lines used a switching scale at $Q^2_{\text{switch}} = 4m_D^2$, and the blue dashed lines uses $16m_D^2$.

Performance – Bulk medium

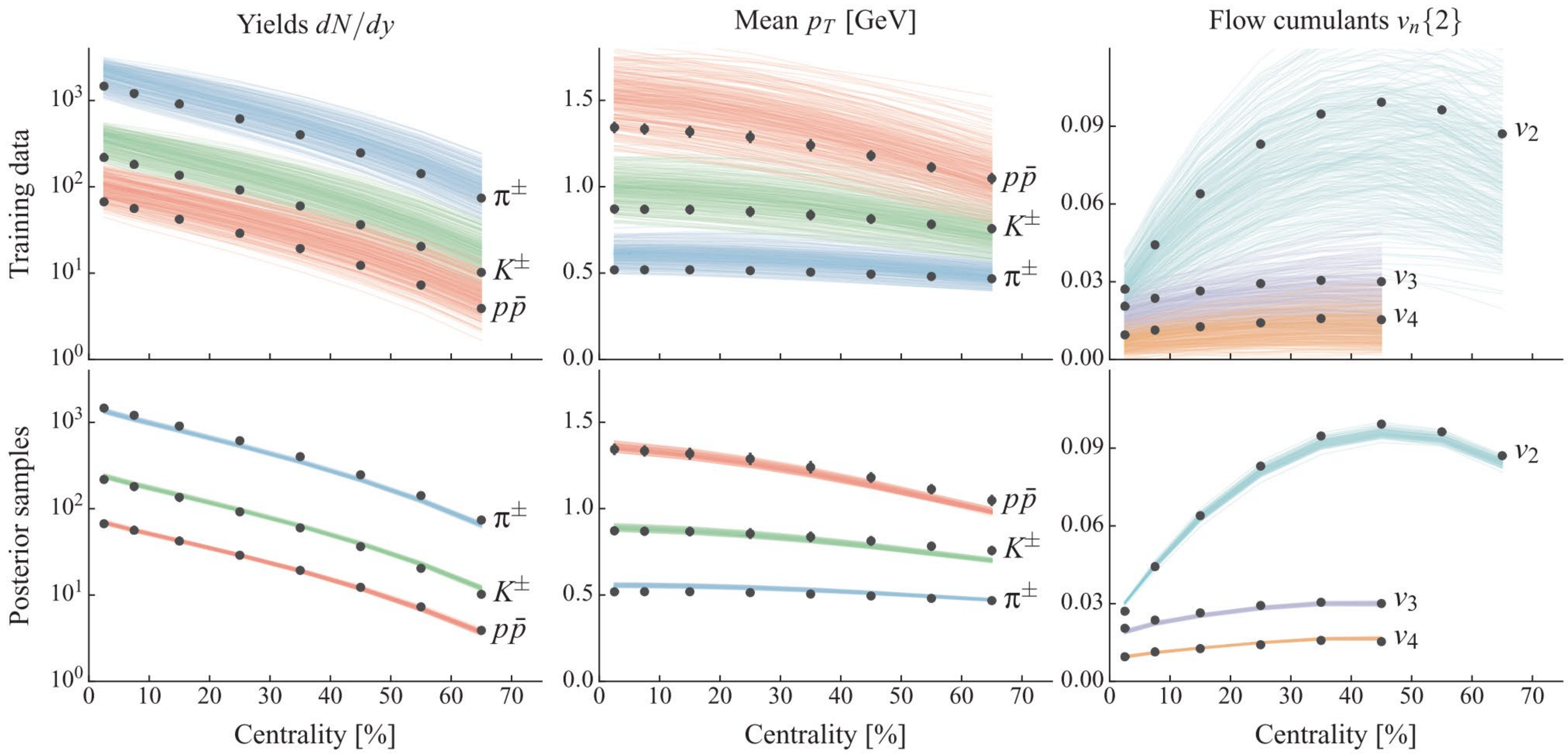

APPENDIX

Performance – Bulk medium

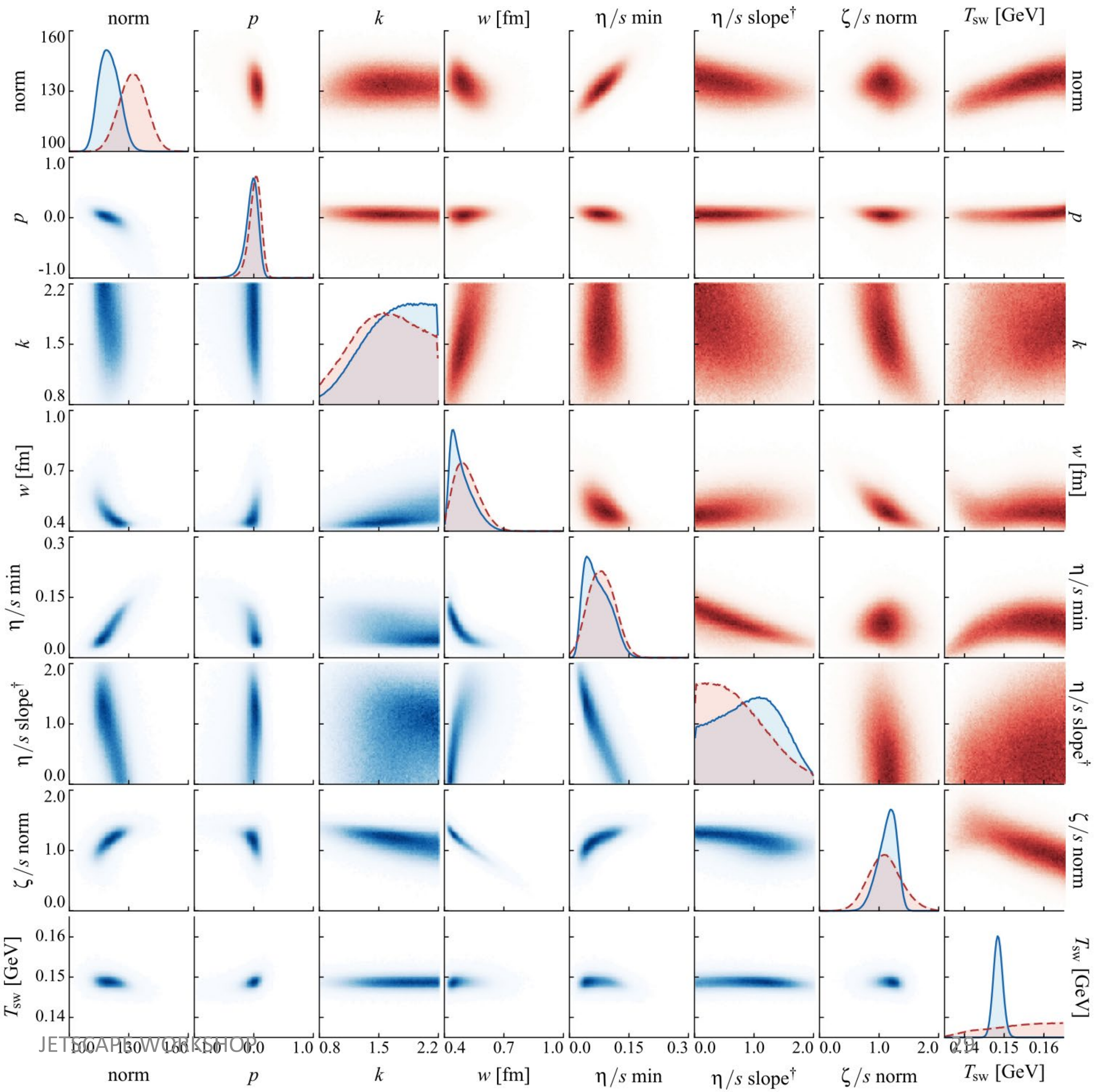

Performance - Lido

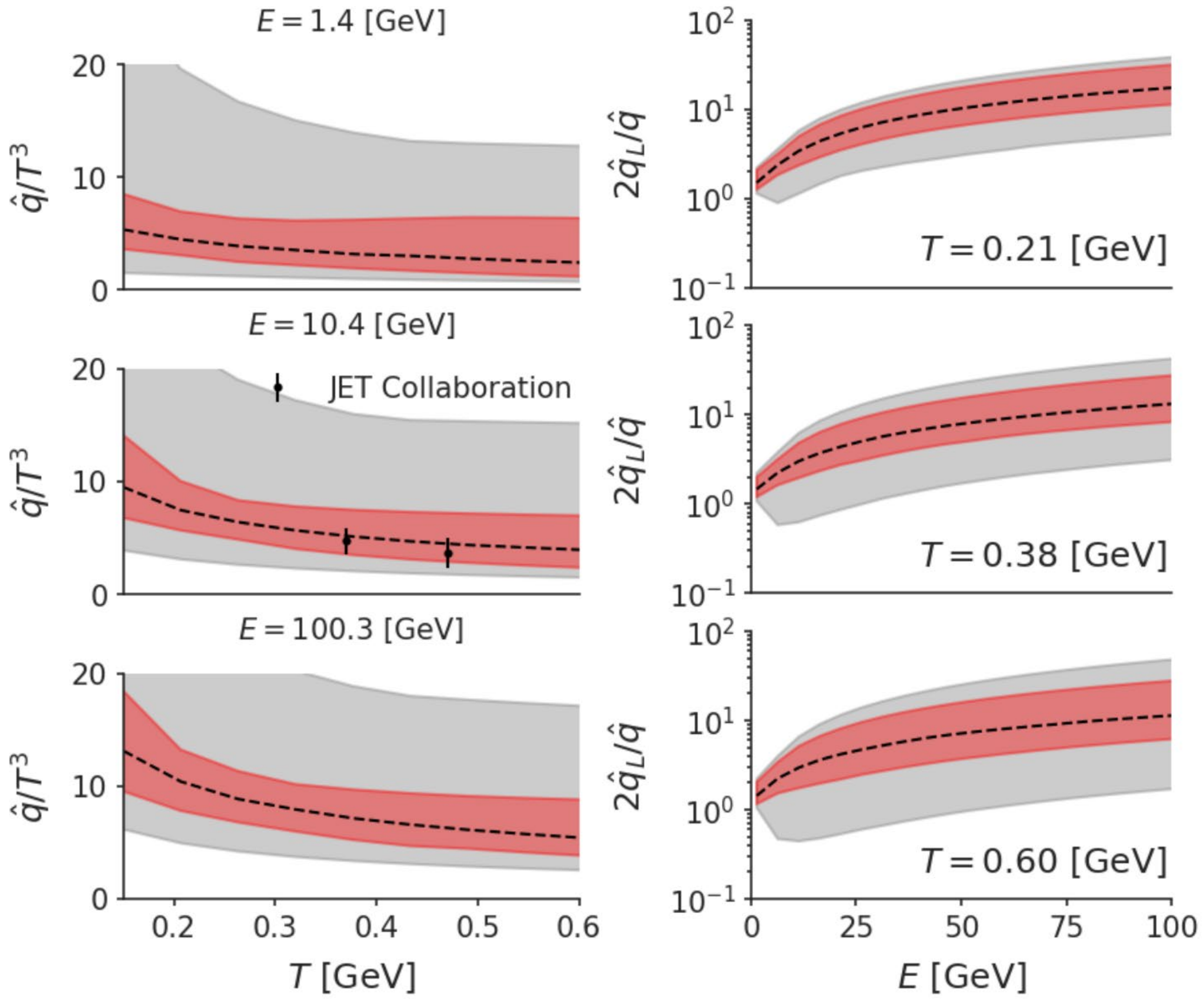

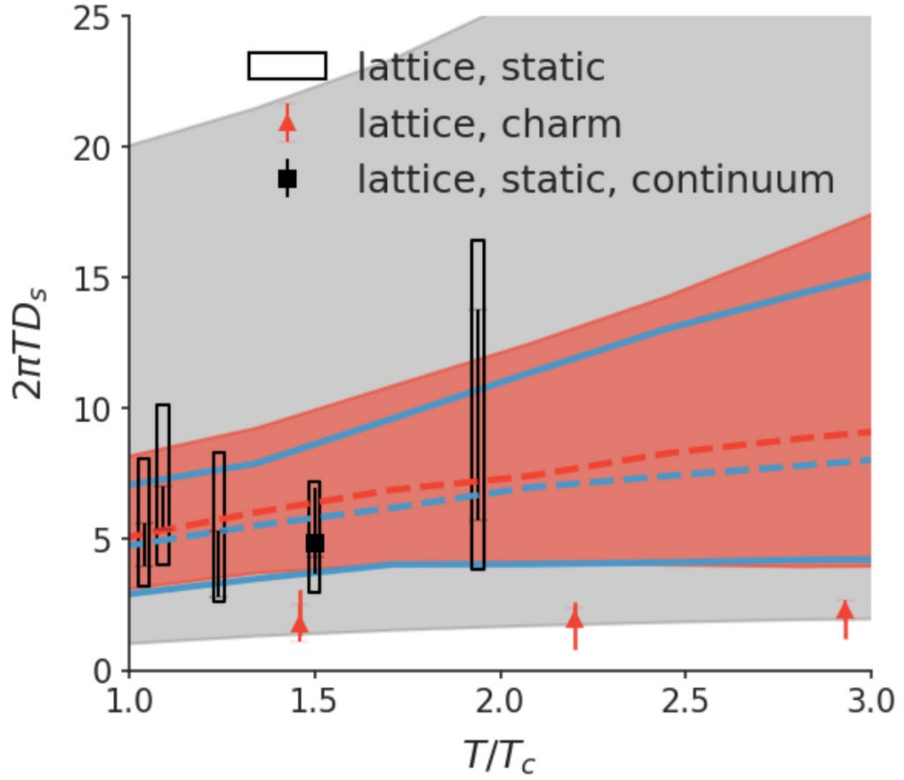

PART 3

Jet and Jet Substructure – Preliminary results

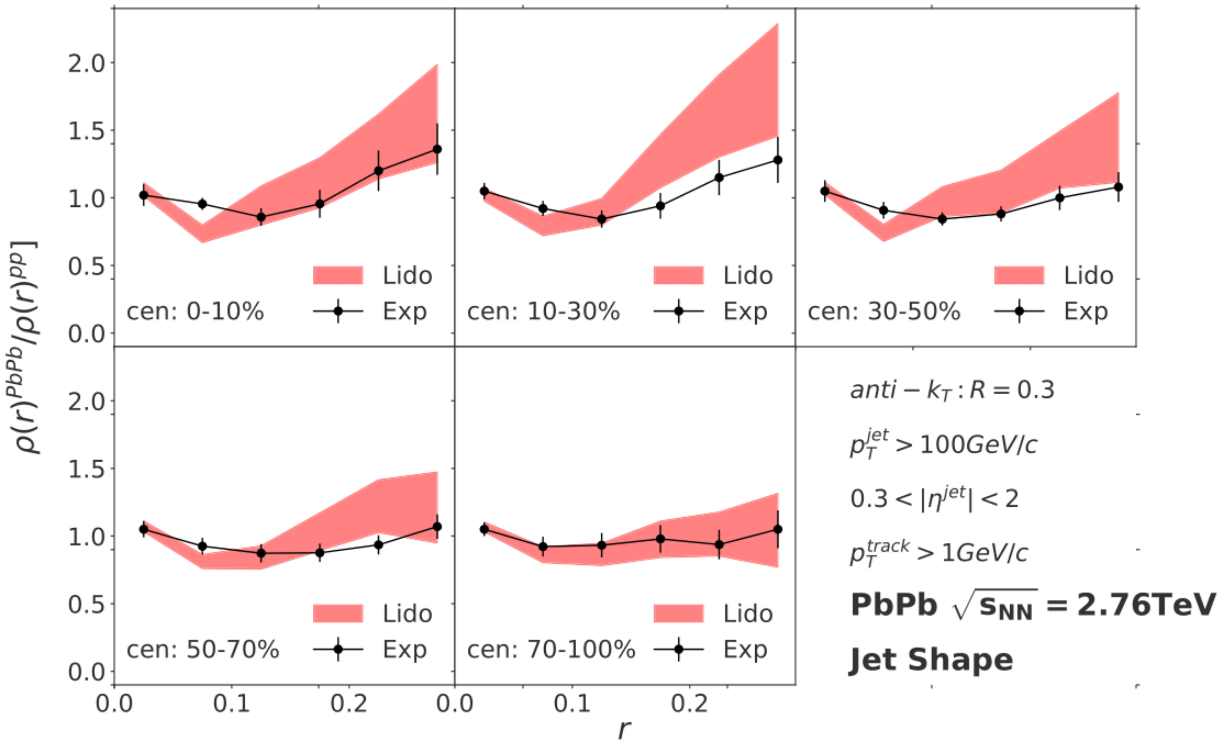

Jet shape with recoil

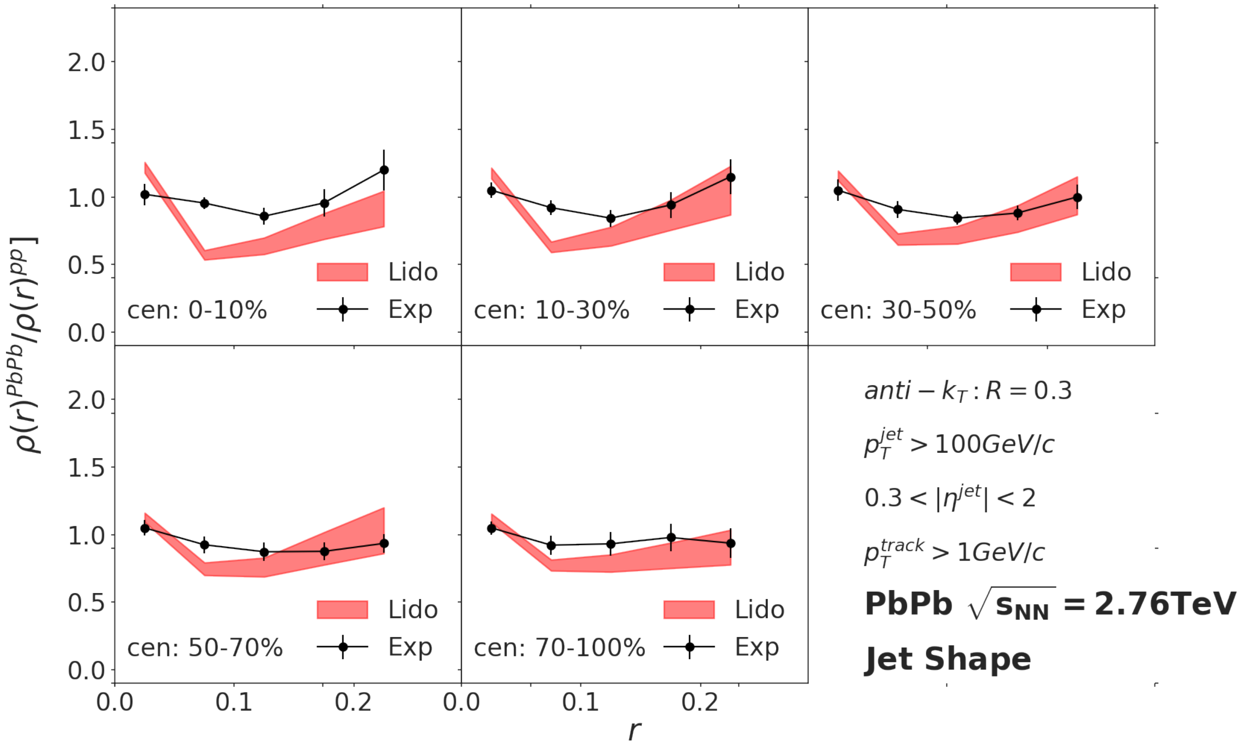

Jet shape without recoil